

SCIENTIFIC REPORTS



OPEN

Human gut derived-organoids provide model to study gluten response and effects of microbiota-derived molecules in celiac disease

Rachel Freire^{1,2}, Laura Ingano¹, Gloria Serena^{1,2}, Murat Cetinbas^{2,3}, Anthony Anselmo^{2,3,4}, Anna Sapone^{1,2,5}, Ruslan I. Sadreyev^{2,3}, Alessio Fasano^{1,2,6} & Stefania Senger^{1,2}

Celiac disease (CD) is an immune-mediated disorder triggered by gluten exposure. The contribution of the adaptive immune response to CD pathogenesis has been extensively studied, but the absence of valid experimental models has hampered our understanding of the early steps leading to loss of gluten tolerance. Using intestinal organoids developed from duodenal biopsies from both non-celiac (NC) and celiac (CD) patients, we explored the contribution of gut epithelium to CD pathogenesis and the role of microbiota-derived molecules in modulating the epithelium's response to gluten. When compared to NC, RNA sequencing of CD organoids revealed significantly altered expression of genes associated with gut barrier, innate immune response, and stem cell functions. Monolayers derived from CD organoids exposed to gliadin showed increased intestinal permeability and enhanced secretion of pro-inflammatory cytokines compared to NC controls. Microbiota-derived bioproducts butyrate, lactate, and polysaccharide A improved barrier function and reduced gliadin-induced cytokine secretion. We concluded that: (1) patient-derived organoids faithfully express established and newly identified molecular signatures characteristic of CD. (2) microbiota-derived bioproducts can be used to modulate the epithelial response to gluten. Finally, we validated the use of patient-derived organoids monolayers as a novel tool for the study of CD.

Celiac disease (CD) is an immune-mediated disorder characterized by an autoimmune enteropathy triggered by gluten intake in genetically predisposed subjects carrying HLA-DQ2 or HLA-DQ8 haplotypes¹. About 1% of the general population is affected by the disease². The enteropathy is characterized by villous atrophy, crypt hyperplasia, and swelling of the lamina propria with infiltration of immune cells, including neutrophils and lymphocytes³. Gluten-specific and tissue transglutaminase (tTG) antibodies are expressed during the acute phase².

Extensive studies have been conducted on gluten, the known trigger for CD. Gluten is composed of gliadins and other storage proteins found in wheat, barley, and rye¹. Gliadin's family has been identified as responsible for CD pathogenesis in multiple ways, exerting cytotoxic, immunomodulatory, and gut-permeating activities on the intestinal mucosa⁴.

Based on current data, it is hypothesized that CD onset is preceded by the following sequence of events: after oral intake, undigested gliadin peptides trigger the release of zonulin, leading to increased intestinal permeability^{5,6}. The disrupted barrier allows translocation of gliadin's peptides to the lamina propria and subsequent interaction with macrophages and other immune cells^{4,7}. Gliadin peptides promote IL8 and IL15 secretion from enterocytes, leading to recruitment of neutrophils⁸ and intraepithelial lymphocytes⁹. Finally, the interaction of T

¹Mucosal Immunology and Biology Research Center and Center for Celiac Research and Treatment, Department of Pediatrics, Massachusetts General Hospital, Boston, MA, USA. ²Harvard Medical School, Boston, MA, USA. ³Department of Molecular Biology, Cancer Center and Center for Regenerative Medicine, Massachusetts General Hospital, Boston, MA, USA. ⁴Present address: PatientsLikeMe, Inc., Cambridge, MA, USA. ⁵Present address: Translational Research and Early Clinical (TREC), GI, Takeda Pharmaceuticals International Co., Boston, MA, USA. ⁶European Biomedical Research Institute of Salerno (EBRIS), Salerno, Italy. Alessio Fasano and Stefania Senger jointly supervised this work. Correspondence and requests for materials should be addressed to S.S. (email: ssenger@mgh.harvard.edu)

cells with gliadin's peptide-presenting cells in a pro-inflammatory milieu leads to the abrogation of oral tolerance and activation of the Th1/Th17 adaptive immune response¹⁰.

The chain of events as hypothesized implies that the interaction between the host and the trigger is necessary and sufficient, suggesting that the onset of CD occurs at the time of the first encounter, namely the introduction of solid, gluten-containing food to at-risk infants. However, epidemiological data suggest that CD onset can occur at any age, even decades after the introduction of gluten into the diet^{11,12}. Therefore, other factor(s) must be at play to dictate “if and when” an individual genetically at risk for CD loses tolerance to gluten. Novel evidence suggests that the gastrointestinal tract microbiota may play a role in the pathogenesis of CD^{13,14}. A proof-of-concept study by Sellitto and co-authors¹⁵ established that infants who were genetically predisposed to CD and went on to develop the disease expressed a dysbiotic microbiota during the preclinical phase of CD. This was characterized by a decreased representation of *Bacteroidetes*, a high abundance of *Firmicutes*, and a peak and the subsequent drop of *Lactobacillus* species. These changes were concurrent with alterations of the microbiota metabolome signature regarding the relative abundance of butyrate and lactate levels¹⁵. Of note, both butyrate and lactate have been shown to exert a relevant role in regulating the ratio between FoxP3 spliced isoforms in T cells and consequent activation of the Th17-driven immune response in CD¹⁶.

Although major efforts have been undertaken to understand the adaptive immune component associated with the physiopathology of CD, little is still known about the early steps leading to loss of gluten tolerance. The lack of a reliable *in vivo* animal model for CD has hampered our scientific progress, which has been mainly generated by *in vitro* studies on whole biopsies, or on immortalized or cancer cell lines¹⁷. Questions remain about antigen trafficking, activation of the innate immune response, and the development of crypt hyperplasia in a person with a genetic background at risk for CD. Furthermore, to date, no studies have defined whether and how gut microbiota composition and derived bioproducts could mechanistically contribute to CD onset. Thanks to recent development of new techniques, it is now possible to generate organoids from human intestine, an important tool for a patient-derived *in vitro* model^{18,19}.

Therefore, in this study, we aimed at harnessing this technology to generate and validate the use of intestinal organoids from patients to investigate the contribution of the intestinal epithelium in CD pathogenesis. We compared the global gene expression in organoids derived from CD and non-celiac (NC) patients to identify differences relevant to the enteropathy. We established a reliable tool to study intestinal epithelial cell permeability, immune function, and epithelium regeneration. Moreover, based on our hypothesis that peculiar profiles of microbiota and their derived bioproducts are mechanistically linked to modifications of gut mucosal functions, we evaluated the effect of bacterial bioproducts in modulating the epithelium's response to gliadin.

Results

RNA sequencing analysis in organoids reveals differences in gene expression potentially relevant to celiac disease pathogenesis. We generated and characterized epithelial organoids derived from duodenal biopsies of NC and CD patients. We aimed at comparing patterns of gene expression in the organoids using RNA sequencing (RNA-seq). Multivariate analyses revealed that the samples grouped together based on their respective diagnosis. While the active CD-derived organoids shared similar transcriptional signatures, the NC sample set appeared more heterogeneous (Fig. 1a). Nonetheless, we found 472 genes differentially expressed (fold change greater than 2, FDR < 0.05) between the two groups. Of them, 291 genes were downregulated and 181 were upregulated in CD compared to NC (Fig. 1b; Supplementary Table S1).

Although CD is an adaptive immune-mediated enteropathy, evidence suggests that changes associated with intestinal functions, including gut permeability and innate immunity, could play a pivotal role in CD onset^{5,9,20}. Furthermore, crypt hyperplasia, a hallmark of CD that occurs during the acute phase, has been associated with the dysregulation of intestinal stem and progenitor cells²¹. To further investigate functional categories among genes that are differentially expressed in CD organoids, we performed DAVID gene ontology analysis (GO)^{22,23}, gene set enrichment analysis (GSEA)²⁴ as well as in-depth manual inspection of differentially expressed genes to identify candidates that could contribute to CD pathogenesis. Among differentially expressed genes, the greatest percentage clustered by terms “extracellular space” and extracellular region” in the category GO cellular component (GOTERM_CC) and “signal” and “secreted” in UP Keywords (Supplementary Table S2). Those genes included stem cell, glycolyx genes and chemokines. Specifically, components of the WNT signaling pathway, including LGR5, OLFM4, SMOC2, ASCL2, EPHB3, and DLL1, were found upregulated in CD organoids, whereas DKK1, a WNT negative regulator²⁵ was significantly downregulated (Fig. 1b; Supplementary Fig. S1). These data are consistent with an overrepresentation of actively proliferating cells, including stem and progenitor cells in CD organoids, and are in line with previous findings in celiac biopsies²¹.

We observed that genes associated with gut barrier functionality such as the pore-forming claudin 2 (CLDN2)²⁶ and the essential scaffolding protein tight junction protein 1 (TJP1; also known as ZO1)²⁷, were respectively up- and downregulated in CD organoids, albeit slightly below the two-fold threshold (fold change 1.9 and 1.55). These results are consistent with previous observations in CD biopsies^{28,29}. Additionally, we identified novel genes that are significantly downregulated in CD organoids, including sealing tight junction protein CLDN18²⁶ and some components of the mucus layer MUC6, MUC5AC, and trefoil factors (TFF1 and TFF2). In addition, genes associated with an innate immune response, such as the chemokines CCL24 and CCL25, the initiator of the inflammasome complex formation NLRP6, the alpha-defensins DEFA5 and DEFA6, and the anti-inflammatory cytokine IL37 were upregulated in organoids from CD patients (Fig. 1b).

To validate the RNA-seq dataset related to the three key biological functions outlined above, quantitative reverse transcription-PCR (qRT-PCR) was performed on a subset of the identified genes in a larger organoid sample set. We confirmed the upregulation of CLDN2 and downregulation of CLDN18, MUC6, MUC5AC, TFF1 and ZO1 in active CD organoids (Fig. 1c). Relatively to innate immunity associated genes, we confirmed the upregulation of all the evaluated genes: IL37, DEFA5, NLRP6, CCL24 and CCL25 (Fig. 1d). Finally, we evaluated the expression of the genes involved in stem cell function and found, consistent with RNA-seq data set, significant upregulation of LGR5, SMOC2 and OLFM4. ASCL2 was found upregulated, but not significantly (Fig. 1e).

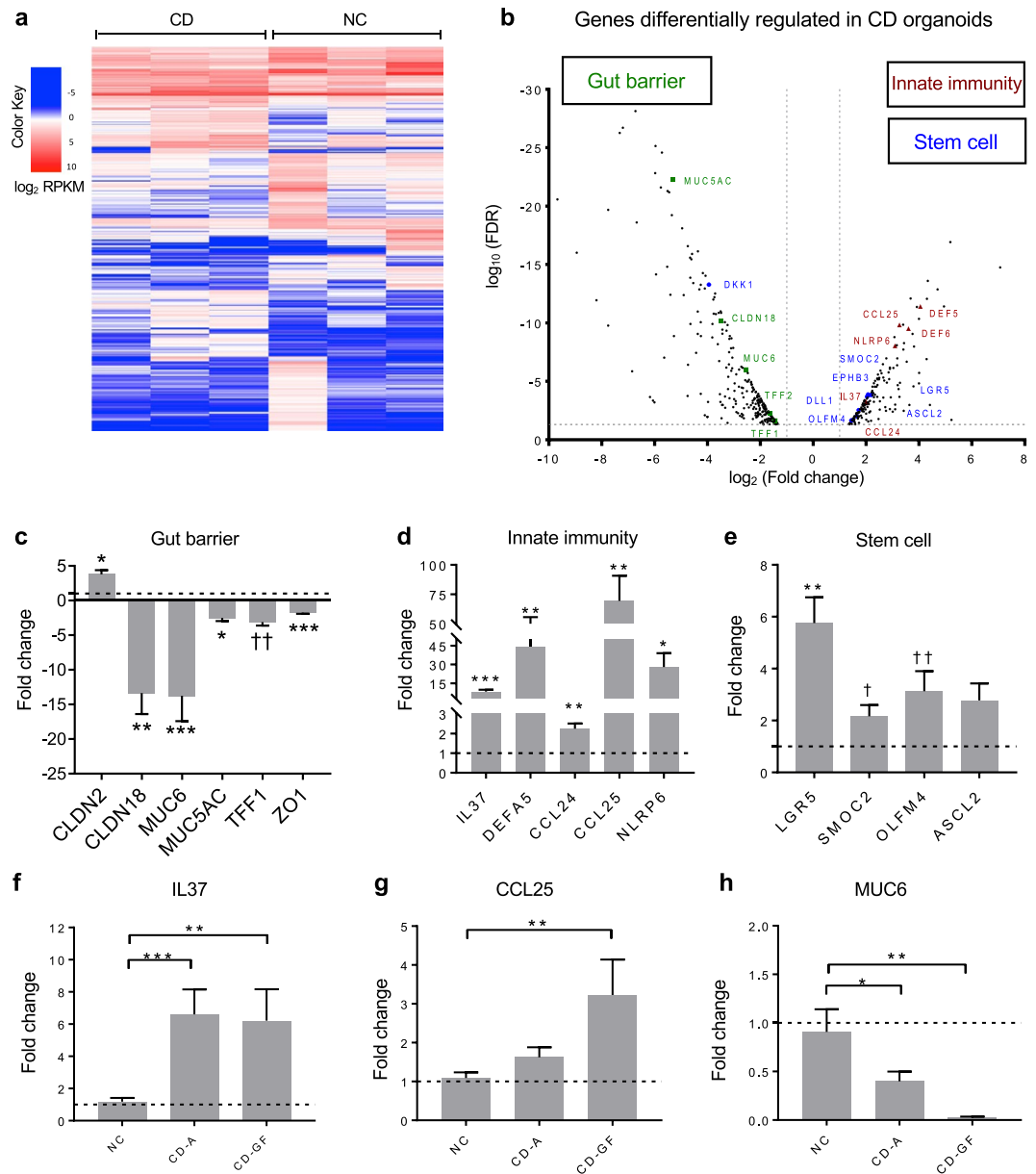


Figure 1. Differential gene expression profiles in active celiac epithelial organoids and human whole duodenal biopsies. **(a)** Heatmap representing RNA-seq expression values (\log_2 RPKM) for the genes differentially expressed in organoids from patients with active celiac disease (CD, n = 3) compared to non-celiac controls (NC, n = 3). A color code from blue to red indicates low and high expression levels, respectively. **(b)** Volcano plot showing fold change (X axis in \log_2 scale) and statistical significance (FDR, Y axis in \log_{10} scale) for differentially expressed genes (RNA-seq) in active celiac (CD, n = 3) compared to non-celiac (n = 3) organoids. Selected differentially expressed genes are highlighted and colored by functional categories associated with gut barrier function (green), innate immunity (red), and stem cell function (blue). **(c–e)** Validation by qRT-PCR of selected genes found differentially expressed in active celiac epithelial organoids by the RNA-seq analysis, belonging to relevant functional categories: gut barrier **(c)**, innate immunity **(d)**, and stem cell **(e)**. Data represent average expression relative to NC control \pm SEM; * $p < 0.05$, ** $p < 0.01$, *** $p < 0.001$, two-side unpaired t-test; † $p < 0.05$, †† $p < 0.01$, Mann-Whitney test; 12 to 18 replicates for n = 5 non-celiac and n = 5 active celiac organoids. **(f–h)** Gene expression assessed by qRT-PCR in human duodenal biopsies of non-celiac (NC, n = 6–11), celiac patients with active disease (CD-A, n = 17), and celiac patients in remission following a gluten-free diet (CD-GF, n = 5–6) to validate the organoid model. Data represent average expression relative to NC \pm SEM. * $p < 0.05$, ** $p < 0.01$, *** $p < 0.001$, Mann-Whitney test.

Studies from our group and others have established that human organoids retain a gene expression program that recapitulates the expression of the tissue of origin, including a diseased state^{19,30}. To substantiate these findings in CD organoids, we evaluated the expression of selected newly identified genes including IL37, CCL25, MUC6, CLDN18 and CCL24 in duodenum biopsies from NC, CD patients with active disease, and CD patients

in remission following a gluten-free diet (GFD). Consistent with the expression in CD organoids, we found that IL37 and CCL25 were upregulated, whereas MUC6 was significantly downregulated in the CD biopsies of both active and in-remission patients (Fig. 1f–h). CCL24 was not differentially expressed, whereas CLDN18 was found upregulated in CD-A duodenum biopsies (Supplementary Fig. S1b).

CD organoids proliferative defects suggest impaired repair functions of the stem cell compartment.

Histological features including crypt hyperplasia and blunting of the villi are the hallmark of active CD characterized by expansion of the immature-cell population and concurring reduction of the mature cells of the villus³¹. These pathological manifestations of the CD intestinal mucosa have been hypothesized to be the consequence of a faulty stem cell compartment that cannot compensate the tissue turnover and/or a consequence of increased epithelium apoptosis^{32,33}. To establish the proliferative capabilities of the epithelium we seeded NC and active CD single cells in matrigel and recorded the growth of organoids over time (Fig. 2a). We found that after 7 days in culture, the average area of CD organoids was significantly smaller compared to NC controls (Fig. 2b). To investigate the cause of reduced organoids growth, we evaluated the cell distribution across different cell cycle phases over time by propidium iodide (PI) staining, followed by FACS analysis in NC and active CD. We found no significant difference after two days in culture (Supplementary Fig. S2a). By day 4 we observed a reduction in cells in S phase in CD (Supplementary Fig. S2b). By day 7 we found significantly less cells in S phase in CD compared to NC (Fig. 2c,d). To further corroborate the observed reduction of cells in S phase, we evaluated the percentage of actively proliferating Ki67⁺ cells by FACS analysis at days 2, 4 and 7. There was no difference by day 2 between the two samples sets, suggesting that a comparable number of proliferative cells were initially plated. Less Ki67⁺ cells in CD samples compared to respective controls was observed as a trend by day 4 and 7 (Fig. 2e). Consistently we found reduced expression of proliferation markers MYC and PCNA in CD samples by day 7 (Fig. 2f,g). To establish a contribution of apoptosis to the reduced growth of the CD organoids, we evaluated the sub-G0/G1 cell population obtained by PI staining³⁴ as a measure of DNA fragmentation associated to apoptosis³⁵, that did not identify with cell debris (Supplementary Fig. 2c,d). We observed comparable frequency of sub-G0/G1 among the two samples sets at all the analyzed time points (Supplementary Fig. S2e). We also evaluated the expression of pro-apoptotic markers TNF receptor TNFRSF25³⁶ and pro-apoptotic gene TP53³⁷, and we did not find any statistically significant difference, even if TNFRSF25 appeared modestly upregulated in CD (Supplementary Fig. S2f). Finally, we performed immunofluorescence of activated caspase-3 on CD and NC organoids at day 7 and we did not observe significant difference between the samples sets (Supplementary Fig. S2g).

Development and functional characterization of gut organoid-derived monolayers from CD patients.

Next, we aimed at developing organoid-derived monolayers to investigate potential physiological and functional differences between the two experimental groups. We first established the haptoglobin (HP) genotype of the organoids employed in this study. Haptoglobin encodes for two alleles, of which HP2 carries a duplication of the 3rd and 4th exons³⁸. The allele HP2, encodes for the HP2 pre-haptoglobin also known as zonulin, that has been shown to be a physiological regulator of tight junctions and it is released upon gluten stimulation^{39,40}. We found that all the organoids had at least one copy of the HP2 allele (HP2-1 or HP2-2 genotype). Two NC and three CD organoids carried two copies of the allele (HP2-2 genotype).

We derived monolayers from NC and active CD-derived organoids, as previously described^{19,41}. NC and CD monolayers developed with different kinetics based on transepithelial electrical resistance (TEER), with CD monolayers showing a significantly lower TEER at 3, 5, 7 and 9 days post seeding compared to NC (Fig. 3a). Furthermore, to evaluate the paracellular permeability in the developing monolayers, we employed two different molecular size neutral probes such as FITC-Dextran 4,000 Da and FITC-PEG 400 Da to measure their passage across the cell monolayers. While CD monolayers were more permeable to FITC-Dextran 4,000 Da at day 3 compared to NC monolayers, they showed comparable paracellular permeability by day 5 to day 9 (Fig. 3b). However, CD monolayers showed significantly higher permeability to the small FITC-PEG 400 after 5, 7 and 9 days in culture compared to NC monolayers (Fig. 3c). We hypothesized that the difference observed in TEER measurements and FITC-PEG 400 could reflect either barrier function and/or maturation impairment, both suggested by the gene expression data set observed in organoids (Fig. 1c–e). Consistent with the gene expression data the immunofluorescence staining of the ZO1 showed less deposition of this protein along the cell perimeter of CD monolayers (Fig. 3d), suggesting defects in barrier deposition.

We further investigated the ability of the cell monolayers to differentiate in absorptive and secretory cells (see Methods). We evaluated the expression of lysozyme (LYZ), sucrase isomaltase (SI), mucin-2 (MUC2) and chromogranin A (CHGA) genes expressed respectively by Paneth's cells, enterocytes, goblet's cells and neuroendocrine cells. We found that LYZ was not differentially regulated in the two samples sets, neither was influenced by culturing conditions (Fig. 3e). As expected, the differentiating media promoted the maturation of enterocytes, goblet cells, and enteroendocrine in both NC and CD (Fig. 3f–h). Nevertheless, we observed a significant upregulation of MUC2 and CHGA expression at baseline and upon differentiation in CD monolayers when compared to NC cell monolayers (Fig. 3g,h).

Gliadin increased intestinal permeability and triggered the release of pro-inflammatory cytokines in CD monolayers only.

Gliadins have been shown to have immunomodulatory and gut-permeating functions⁴. A peptic-tryptic digest of α -gliadin (PTG) induced a significant increase in intestinal permeability in both biopsies and adenocarcinomas cell lines^{5,6}, and in pro-inflammatory cytokine secretion^{8,42}. We sought to study the response of CD and NC monolayers to PTG. The PTG was generated as previously reported⁴³ and baseline cytotoxicity (Supplementary Fig. S3c) and endotoxin content was evaluated (see Methods).

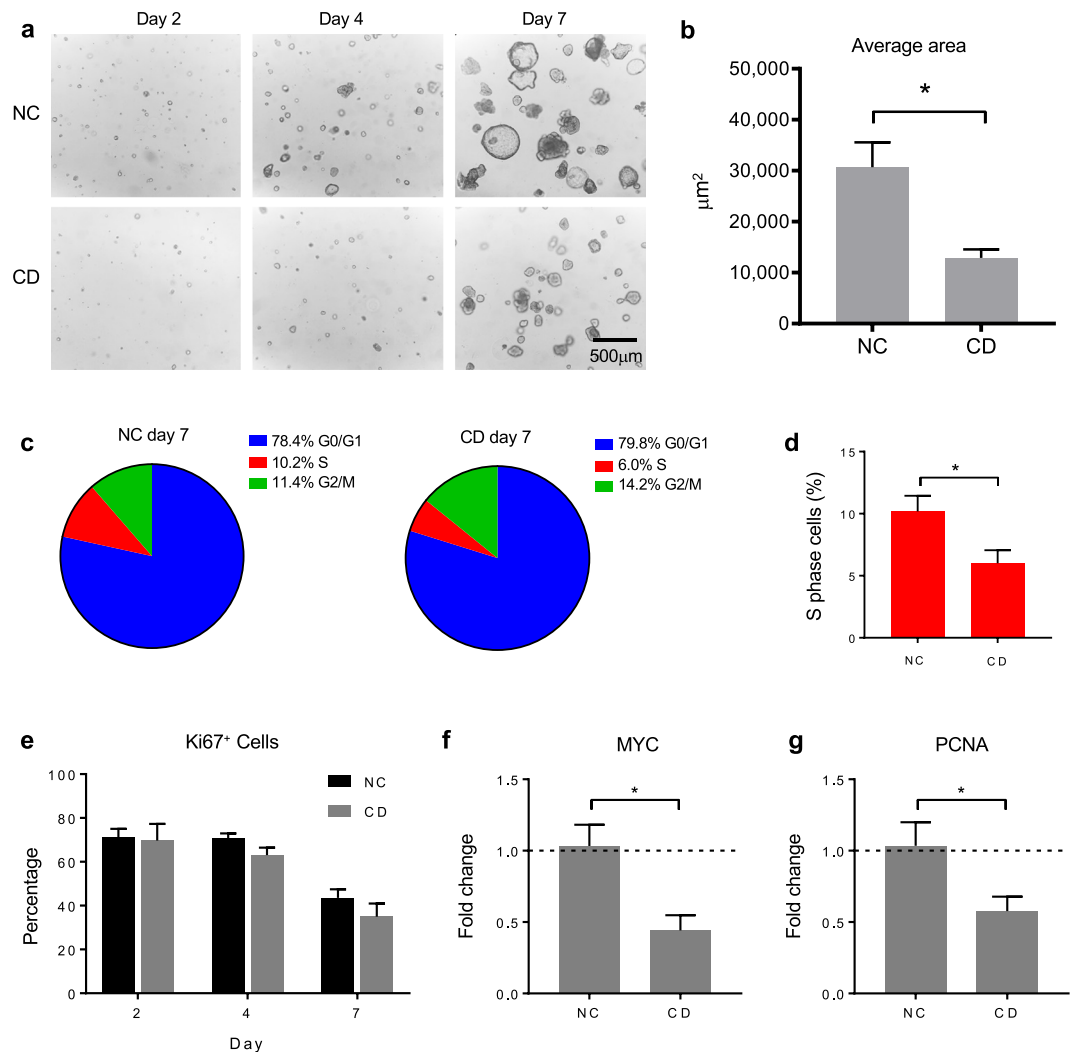


Figure 2. Development and proliferation of non-celiac and active celiac organoids over time. **(a)** Representative images of one non-celiac (NC) and one active celiac (CD) epithelial organoids' growth in matrigel 2, 4 and 7 days after plating. Cells were seeded at 5×10^4 cells/mL density. **(b)** Averaged area (μm^2) of organoids measured from microscopic image of $n = 4$ non-celiac (NC) and $n = 3$ active celiac (CD) patients, 7 days after seeding. ImageJ was used to calculate the area of 42 to 132 organoids for NC and 69 to 129 organoids for CD. Total area of the field is equal to $1.17 \times 10^7 \mu\text{m}^2$. Data represent average \pm SEM. $*p < 0.05$, Mann-Whitney test. **(c)** Pie charts representing the percentage of cells in G0/G1 phase (blue), S phase (red) and G2/M phase (green) in non-celiac (NC, $n = 4$) and active celiac (CD, $n = 4$) organoids as determined by propidium iodide staining after 7 days in culture. Cells percentages were calculated out of gated cells that excluded debris, doublets and apoptotic cells. **(d)** Percentage of cells in S phase in non-celiac (NC, $n = 4$) and active celiac (CD, $n = 4$) organoids as determined by propidium iodide staining after 7 days in culture. Data represent average \pm SEM. $*p < 0.05$, Mann-Whitney test. **(e)** Percentage of proliferating cells established by Ki67⁺ marker in non-celiac (NC, $n = 4$) and active celiac (CD, $n = 4$) organoids over time (day 2, 4 and 7). Double positive Ki67⁺H3P⁺ cells were excluded because represented mitotic cells. **(f,g)** Gene expression assessed by qRT-PCR in non-celiac (NC, $n = 4$) and active celiac (CD, $n = 3$) organoids. Data represent average expression relative to NC \pm SEM. $*p < 0.05$, Mann-Whitney test.

We aimed at evaluating the effect of PTG on tight junction functionality by challenging the monolayers derived from NC and CD organoids. PTG was apically administered to the monolayers for 4 hours. We found that the treatment with PTG increased the paracellular permeability of CD monolayers, based on FITC-dextran 4,000 Da paracellular passage (Fig. 4a), whereas did not affect paracellular permeability of NC monolayers. Furthermore, we evaluated the immune response of PTG treated monolayers. We selected a panel of five pro-inflammatory cytokines to be assessed in the basolateral supernatant. Based on previous reports we evaluated IL8 and IL6, which were found to be significantly upregulated in biopsies or Caco-2 cells treated with PTG^{8,42}. We expanded our analysis to other pro-inflammatory cytokines critical for CD pathogenesis including IL15, which is relevant for the recruitment of intraepithelial lymphocytes⁹ and TNF and IFN γ , which are detrimental to intestinal integrity⁴⁴. We found that PTG significantly stimulated the secretion of IL6 in both NC and CD monolayers, whereas it triggered a significant release

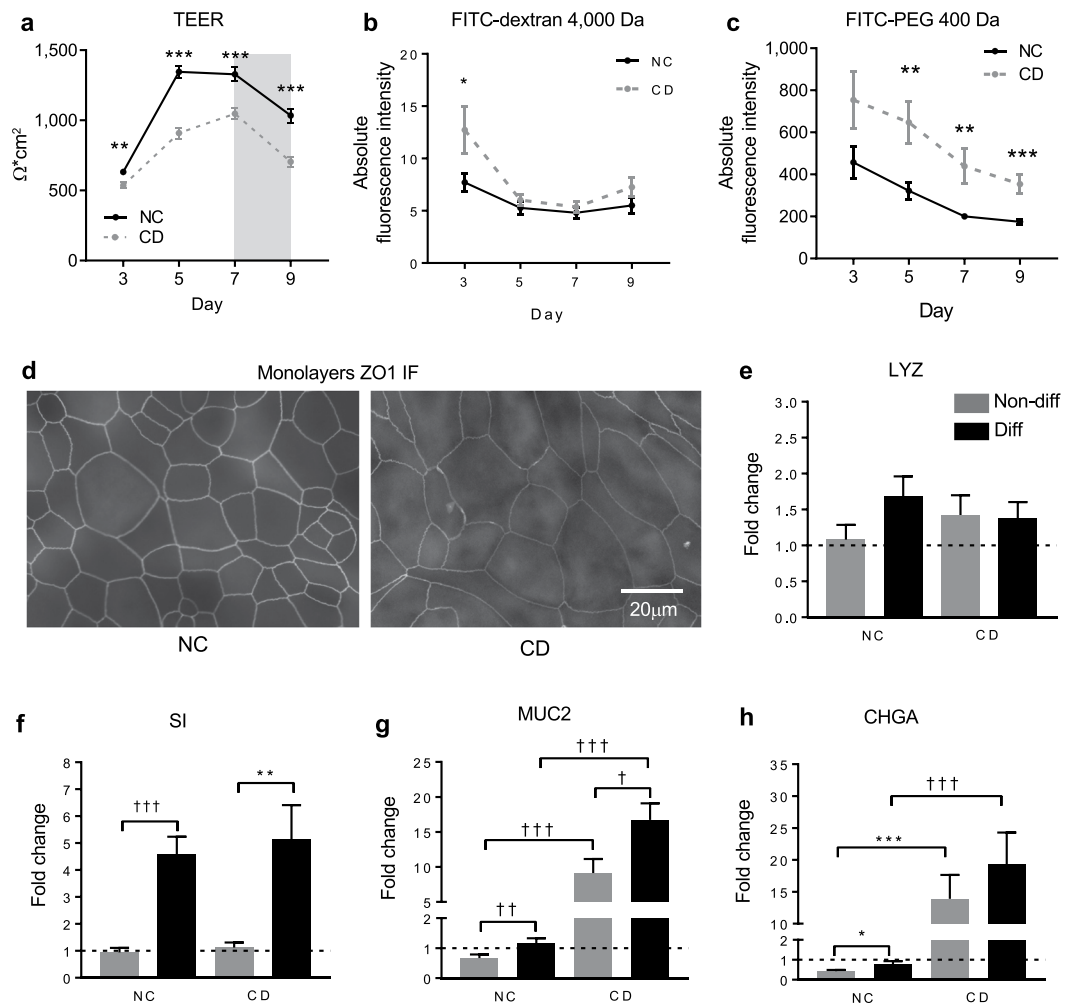


Figure 3. Development of non-celiac and celiac organoid-derived monolayers. **(a)** Transepithelial electrical resistance (TEER) measurement to evaluate development of the monolayers over time. Data represent average \pm SEM. $**p < 0.01$, $***p < 0.001$, two-side unpaired test; 149 to 234 replicates for $n = 5$ non-celiac (NC) and 156 to 253 replicates for $n = 5$ active celiac (CD) organoid-derived monolayers. **(b,c)** Absolute fluorescence intensity of FITC-dextran of 4,000 Da **(a)** and FITC-PEG of 400 Da **(b)** recovered in the basolateral side after 4 h of incubation. Data represent average \pm SEM. **(b)** $*p < 0.05$, two-side unpaired t-test; 12 replicates for $n = 4$ non-celiac (NC) and $n = 4$ active celiac (CD) at each time point. **(c)** $**p < 0.01$, $***p < 0.001$, two-side unpaired t-test; 12 and 9 replicates for $n = 4$ non-celiac (NC) and $n = 3$ active celiac (CD) at each time point. **(d)** Immunofluorescence staining of TJP1 (also known as ZO1) performed on one representative non-celiac (NC) and one active celiac (CD) monolayer at day 7 showing reduced deposition of the tight junction protein along the apical cell perimeter. **(e–h)** Gene expression assessed by qRT-PCR in organoid-derived monolayers cultured in two differentiation conditions (see Methods). LYZ **(e)**, SI **(f)**, MUC2 **(g)** and CHGA **(h)** evaluated the relative abundance of Paneth's cells, enterocytes, goblet's cells and neuroendocrine cells, respectively. Data represent average expression relative to NC non-differentiated \pm SEM. $*p < 0.05$, $**p < 0.01$, $***p < 0.001$, two-side unpaired t-test. $\dagger p < 0.01$, $\dagger\dagger p < 0.001$ Mann-Whitney test; 20 and 16 replicates for $n = 4$ non-celiac (NC) and $n = 3$ active celiac (CD) patients.

of $\text{IFN}\gamma$, TNF, IL15 and IL8 cytokines only in the CD monolayers (Fig. 4b). The PTG negative control (PTG-CT) did not affect the release of any of the analyzed cytokines (see Methods; Supplementary Fig. S3b).

Microbiota-derived bioproducts modified CD epithelium response. Intestinal dysbiosis has been reported in CD and other intestinal inflammatory diseases^{13,45}. Additionally, a microbiota imbalance has been claimed to be associated with CD onset¹⁵.

We aimed at evaluating whether microbiota-derived molecules (bioproducts) could exert a protective role on the epithelial functions critical to the development of CD. Based on previous observations¹⁵ and as a proof of concept, we decided to analyze the effect of butyrate, lactate, and polysaccharide A (PSA). This last bioproduct, which holds recognized immunoprotective activity^{46,47}, was derived from *Bacteroides fragilis*. The concentration of metabolites used reflected physiological levels in non-dysbiotic individuals relatively to butyrate and lactate¹⁵. PSA was evaluated at concentration previously adopted in other cellular models⁴⁸.

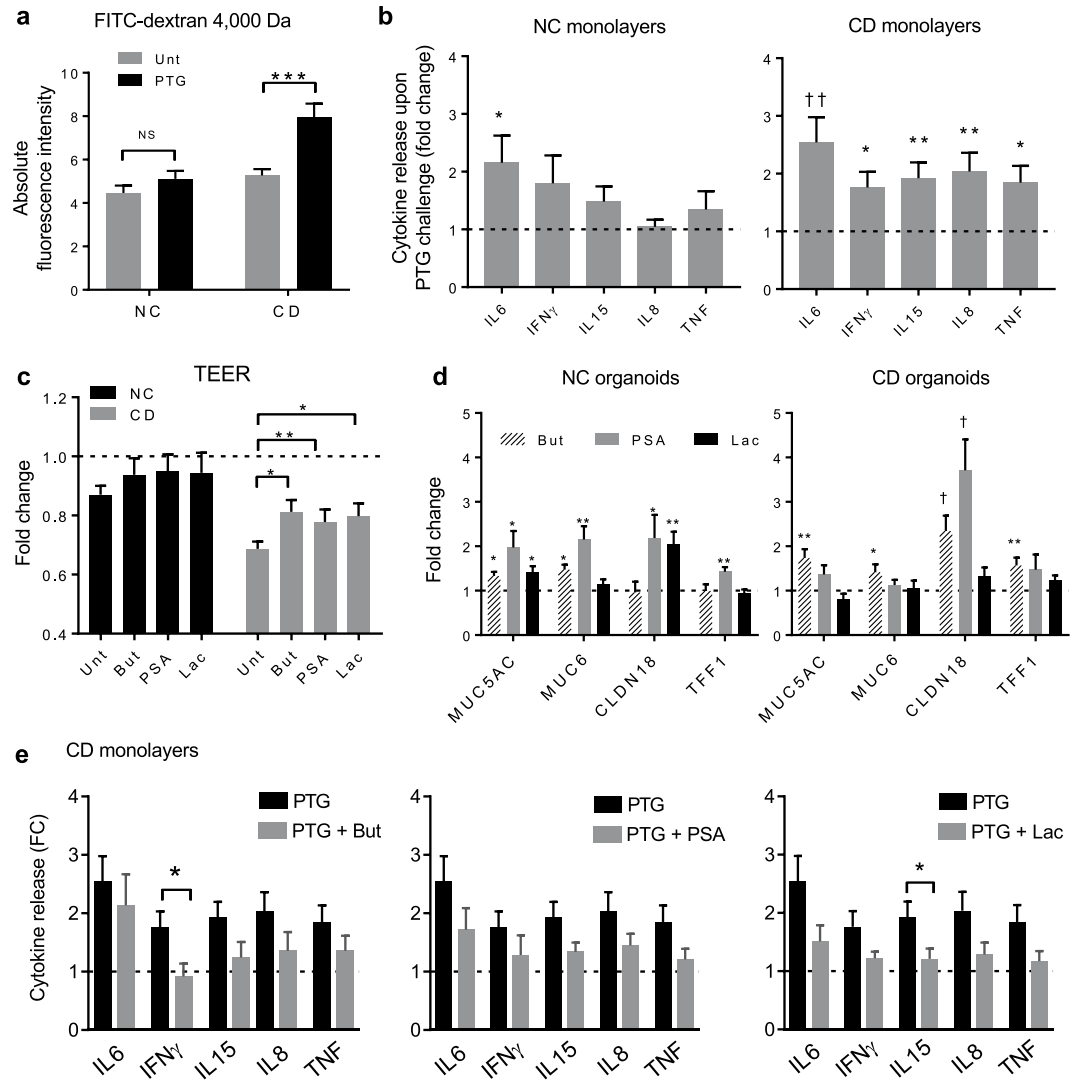


Figure 4. Effects of gliadin, butyrate, PSA and lactate on barrier function and pro-inflammatory cytokines. **(a)** Absolute fluorescent intensity of FITC-dextran 4,000 Da recovered in the basolateral side of confluent monolayers after 4 h incubation with 1 mg/mL pepsin-trypsin digested-gliadin (PTG) or media control (Unt). Data represent average \pm SEM. *** $p < 0.001$; Mann-Whitney test; 21 to 30 replicates for $n = 5$ non-celiac (NC) and $n = 6$ celiac (CD) patients. NS: not-significant. **(b)** Secreted cytokines measured by ultra-sensitive multiplex electrochemiluminescence in the basolateral supernatants of non-celiac (NC) and celiac (CD) monolayers upon 4 h challenge with 1 mg/mL PTG. Fold change calculated relative to untreated monolayers. Data represent average \pm SEM. * $p < 0.05$, ** $p < 0.01$, two-side unpaired t-test. †† $p < 0.01$, Mann-Whitney test; 10 to 15 replicates for $n = 5$ NC and $n = 6$ CD patients. **(c)** Fold change of transepithelial electrical resistance (TEER) measured in non-celiac (NC) and celiac (CD) confluent monolayers after 48 h treatment with butyrate (But), polysaccharide A (PSA) or lactate (Lac), expressed as fold change of TEER reading at time 0. Unt: untreated. Data represent average \pm SEM. * $p < 0.05$, ** $p < 0.01$, Mann-Whitney test; 44 to 102 replicates for $n = 5$ NC and $n = 6$ CD patients. **(d)** Expression of genes related to gut barrier function assessed by quantitative RT-PCR in epithelial organoids derived from non-celiac (NC) and celiac (CD) patients, after 48 h treatment with butyrate (But), polysaccharide A (PSA) or lactate (Lac). Data represent average expression relative to untreated \pm SEM. * $p < 0.05$, ** $p < 0.01$, two-side unpaired t-test; † $p < 0.05$, Mann-Whitney test. 8 to 12 replicates for $n = 4$ NC and $n = 4$ CD patients. **(e)** Secreted cytokines measured by ultra-sensitive multiplex electrochemiluminescence in the basolateral supernatants of celiac (CD) monolayers. Monolayers were 48 h pre-treated with microbiota derived-bioproducts butyrate (But), polysaccharide A (PSA) or lactate (Lac) and subsequently challenged with 1 mg/mL PT-gliadin (PTG) for 4 h. Fold change (FC) calculated relative to untreated monolayers. Data represent average \pm SEM. * $p < 0.05$, Mann-Whitney test (PTG vs. PTG pretreated with the bioproducts); 12 to 15 replicates for $n = 6$ (CD) patients.

CD and NC organoids were treated for 48 h with the three bioproducts, and their effect on epithelial barrier functionality was evaluated by measuring TEER and gene expression. Initially, we found that all three of the bacteria-derived bioproducts significantly ameliorated TEER changes in CD (Fig. 4c). Thus, we analyzed the

expression of genes related to gut barrier function, found altered in CD data set (Fig. 1b,c). We found that butyrate significantly upregulated the expression of MUC5AC, MUC6, TFF1 and CLDN18, in CD organoids. PSA significantly increased the expression of CLDN18 only, while lactate did not alter the expression of the analyzed gut barrier function-associated genes. Similar regulation of genes was observed in NC organoids (Fig. 4d).

Finally, we analyzed the effect of the bacterial bioproducts on cytokines released by the CD monolayers challenged with gliadin. We observed that all bioproducts exerted a global protective effect by reducing the pro-inflammatory cytokine secretion triggered by PTG. However, only lactate and butyrate significantly reduced the secretion of IL15 and IFN γ cytokines, respectively in CD (Fig. 4e). In NC monolayers, IL6 secretion was also reduced by all the bioproducts however not significantly (Supplementary Fig. S3d).

Discussion

With this study, we have provided novel functional and molecular data on the contribution of the intestinal epithelium to CD pathogenesis. We have paid particular attention to the effects triggered by the interaction between the host epithelium and environmental factors involved in CD pathogenesis, including causal relationship between microbial effectors (bacterial bioproducts), environmental triggers (gluten), and gene variants (host) leading to CD.

The intestinal epithelium plays a recognized and critical role in the development of CD and other autoimmune diseases⁴⁹. It provides a physical barrier against pathogens and toxins, senses the presence of luminal pathogens, coordinates antigen trafficking, modulates the response of resident immune cells, and dynamically interacts with gut microbiota⁵⁰.

To pursue our objectives, we have generated organoids from the epithelial component of the duodenum of NC and CD patients. By whole transcriptome analysis we have identified 472 genes differentially regulated between the samples sets. Furthermore, we have shown that selected genes identified by RNA-seq in the active CD organoid samples were similarly differentially regulated in whole CD biopsies. These data are consistent with previous observations^{30,51} and provide additional evidence that organoids recapitulate the gene expression profile of the epithelium of origin. Among the differentially expressed gene sets, we have identified novel genes associated with relevant epithelial functions potentially related to CD pathogenesis, namely gut barrier, regeneration (stem cells) and innate immunity. Relative to barrier function-associated genes, we have identified the tight junction protein CLDN18 and the mucin components (MUC6 and MUC5AC) that were significantly downregulated in CD epithelium. Moreover, we found that, consistent with previous studies, CD organoids have upregulated expression of pore-forming CLDN2²⁹, downregulated expression of the tight junction protein ZO1²⁸ and the mucus stabilizer factor TFF1⁵¹. These gene expression data suggest a constitutive defect of barrier functionality in CD, as previously hypothesized^{29,52,53}. In line with the molecular data, we have also demonstrated that CD epithelia have a higher paracellular permeability at baseline, in the absence of a challenging agent (gluten).

Furthermore, we have shown that epithelia from active CD have impaired capabilities to proliferate, but not altered apoptosis at baseline. Our data suggest that on average CD organoids have less cells undergoing S phase, that reflects on slower growth, compared to control. We have also observed a modest increase in the percentage of cells in G2/M phase in CD. Whether the impaired proliferation is the consequence of a slower mitosis needs further investigation. Our data generated *in vitro* are consistent with longitudinal studies on mucosal healing in patients on a GFD. Although most celiac patients are able to fully recover the tissue damage after long term GFD (8 years), about 13% show only mucosal improvement and 6% had persistent villus atrophy⁵⁴. What are the factors that promote the “resetting” of the stem cells back to normal, upon the acute insult, leading to mucosal recovery are not known yet and represent an exciting field for further investigation. Understanding these processes might be beneficial for those patients that do not fully recover from the mucosal damage even after long term GFD.

We have also reported that the analyzed cohort of active CD organoids has altered capabilities of differentiating. CD organoids overexpress stem-related and Paneth cells specific genes, suggesting that organoids from active CD patients express a crypt-like phenotype, in other words, contain more immature cells and that the crypt-like phenotype is independent on the insult (gluten).

The characterization of the cell monolayers has further corroborated the evidence of altered cell maturation in CD. Both NC and CD differentiated the absorptive lineage comparably. However, we identified significant differences in the secretory lineage signature. We observed upregulation of secretory-specific goblet's cell marker MUC2. These data are consistent with previous observations on isolated intestinal epithelium from active CD^{51,55}. Similarly, we found upregulation of CHGA in CD monolayers. CHGA is specifically expressed by enteroendocrine cells and to our knowledge its upregulation in CD has not been previously reported.

Finally, we have explored the immune profile of CD epithelia. We uncovered novel immune-related genes not previously identified, such as CCL25 and IL37 significantly upregulated in CD organoids. The chemokine CCL25 promotes the recruitment of immune cells such as macrophages⁵⁶ and dendritic cells⁵⁷. CCL25 overexpression has been reported in ulcerative colitis⁵⁸. While its involvement in CD has been hypothesized⁵⁹, to our knowledge, it has never been previously shown. We also uncovered that CD organoids overexpressed IL37, an anti-inflammatory cytokine related to chronic inflammation and autoimmune diseases⁶⁰. Of note, IL37 has been found upregulated in systemic lupus erythematosus⁶¹, inflammatory bowel disease⁶², and rheumatoid arthritis⁶³, and it has been shown to inhibit both innate and adaptive immunity⁶⁴. We can speculate that the upregulation of IL37 might reflect a general, adaptive protective mechanism, common to multiple autoimmune diseases, to compensate for a system more prone to inflammation. Moreover, both IL37 and CCL25 upregulation were also confirmed in CD biopsies. Finally, we also confirmed the upregulation of NLRP6, initiator of the inflammasome complex formation⁶⁵ that was previously found overexpressed in epithelial cells isolated from biopsies of CD active patients⁵¹.

Because we provided evidence that organoids faithfully recapitulated the epithelium of origin, we aimed at employing organoid-derived monolayers to gain insights on the functional responses of epithelia from CD patients to gliadin. Gliadins are prolamins responsible for cytotoxic, immunomodulatory, and gut-permeating activities of gluten⁴. Previous studies have shown that a peptic-tryptic digest of gliadin (PTG) augmented intestinal permeability in Caco-2 monolayers⁵ and human intestinal explants⁶. In this study, we have adopted a similar PTG challenge for monolayers from NC and CD organoids. Comparable HP2 genotypes ensured that there was not genetic bias in terms of the tight junctions' modulation by zonulin across the sample sets tested^{5,39}. Our results showed that PTG increased intestinal paracellular permeability in CD monolayers only. Conversely, PTG did not affect permeability in NC-derived monolayers. These data provide, for the first time, evidence of significant epithelial functional differences between CD and NC epithelia in response to gliadin, an observation not previously anticipated based on data generated in adenocarcinoma cell lines⁵.

We have further investigated the profile of cytokines secreted by the epithelia exposed to PTG. Multiple studies have shown that gliadin promotes the secretion of pro-inflammatory cytokines. Intestinal epithelial cells Caco-2/TC7 that were stimulated with PTG secreted IL6⁴², whereas, contrasting data have been generated relative to IL8⁸.

Consistent with previous observations⁵, we found that PTG triggered the release of IL6 in both CD and NC monolayers. However, PTG caused significant secretion of pro-inflammatory cytokines IL8 in CD epithelia only. We also explored the secretion of other biologically relevant cytokines like IL15, IFN γ and TNF. The cytokine IL15 has been shown to be overexpressed in CD patients⁶⁶ and is expressed by intestinal epithelia⁶⁷. Importantly, IL15 plays a central role in CD pathogenesis⁶⁸ by promoting dysregulation of multiple immune mechanisms, by recruiting intraepithelial lymphocytes⁹ and activating Th1 cytokine production (IFN γ and TNF)⁴⁴. We found that IFN γ , TNF, and IL15 were significantly more secreted in CD organoid-derived monolayers only upon gliadin stimulus. These last data further support functional differences between CD and NC epithelia relative to PTG challenge. Importantly, our results provide novel evidence for the use of CD patient-derived organoids as a tool for the identification and the study of agents targeting CD-specific reactions to gluten.

Finally, we sought to establish whether other environmental factors, along with gluten and host genetics, could contribute to or sustain the pathogenesis of the disease. A large number of studies have suggested the involvement of gastrointestinal microbiota in the pathogenesis of CD⁴⁵ and other autoimmune diseases⁶⁹. Nevertheless, most of these studies merely showed correlation and not mechanistic causation between microbiota composition and disease status. In this study, we selected three bacterial bioproducts to be analyzed: butyrate, lactate, and PSA from *B. fragilis*. Our rationale was based on previous observations showing significant alterations of the bacteria phyla producing them and/or their relative abundance (butyrate and lactate) in the preclinical phase of CD¹⁵.

The effects of butyrate on eukaryotic cells have been extensively reported. Specifically, butyrate plays an important regulatory role on transepithelial ion transport⁷⁰, ameliorates mucosal inflammation⁷¹, reduces IFN γ signaling⁷², and ameliorates loss of gut barrier function by increasing the sealing tight junction proteins⁷³. Lactate is the major product of several bacterial families with probiotic properties including *Lactobacilli* and *Bifidobacteria*⁷⁴. These bacteria have been shown to be beneficial for the prevention and treatment of gastrointestinal diseases including CD⁷⁵. Specifically, *Lactobacillus* protects epithelial cells against the harmful effects of TNF and IFN γ ⁷⁶. Finally, studies on PSA suggest that it prevents intestinal inflammatory disease by promoting the differentiation of regulatory cells (Treg) and enhancing IL10 production⁷⁷. In necrotizing enterocolitis (NEC), PSA inhibits IL1 β -induced IL8 inflammation in a fetal intestinal epithelial cell line (H4 cells)⁴⁷.

Given the important role that these three bacterial bioproducts play in maintaining intestinal homeostasis, we evaluated their effects on CD epithelial barrier and immune functions at the baseline and upon gluten challenge. We found that treatments with all the bacterial bioproducts improved the barrier functionality of CD epithelia. These functional data correlated with the upregulation of mucins (MUC5AC and MUC6), TFF1 and CLDN18 expression, genes that were found significantly downregulated in the CD organoid cohort. Consistent with previous data, butyrate was the most biologically active in promoting barrier function. Relative to the CD innate immune response to gluten, we found that lactate and butyrate significantly reduced the gliadin-induced secretion of IL15 and IFN γ . Taken together, our observations indicate that the investigated bacterial bioproducts have a positive impact on barrier function and might exert a protective role in terms of mitigating an immune response to gliadin.

To summarize, our study has provided evidence that CD epithelium express stable transcriptional differences potentially relevant to develop and/or sustain the enteropathy. The molecular data have been further supported by our functional observations in CD-derived monolayers. These novel findings proved further insight in the early steps of CD pathogenesis that were poorly defined so far amid the lack of robust experimental models. Furthermore, we have shown that microbiota-derived bioproducts are promising factors to improve the barrier functionality of the epithelium and to reduce the gliadin-induced pro-inflammatory profile in CD. Finally, we have validated the use of *in vitro* patient-derived organoids to model CD pathogenesis to further study CD treatment and prevention.

Methods

Isolation of duodenal crypts and establishment of culture of human organoids. Duodenal biopsies from NC (n = 5) and CD (n = 6) patients were collected by upper endoscopic procedure performed for routine diagnosis or clinical follow-up. CD diagnosis was confirmed by histopathologic analysis and levels of tTG IgA blood antibodies, whereas NC patients presented normal duodenal mucosa with no evidence for CD. Patients in both groups had comparable average age (NC = 56.2 \pm 13.3 years and CD = 54.6 \pm 20.6 years) and gender distribution, with female donors in the majority (70%).

After collection, biopsies were immediately placed in ice-cold DMEM/F12 complete medium and processed for isolation of intestinal epithelial cells or frozen for further gene expression analysis. The isolation of intestinal

epithelial cells was performed as previously described^{18,19,41}. The duodenal organoids' culture was passaged every 7–9 days using a standard, trypsin-based cell dissociation protocol. About 2×10^6 cells/mL singles were re-plated in matrigel supported by L-WRN/ISC medium¹⁹ and kept at passages ranging from P5 to P22.

Preparation of reagents. A peptic-tryptic digest of gliadin (PTG) was generated by sequential digestion with pepsin and trypsin as previously described⁴³ with the following modification. Briefly, gliadin from wheat (#G3375, Sigma-Aldrich) was dissolved in 5% formic acid at 1 mg/mL and digested with pepsin (#P6887, Sigma-Aldrich) at an enzyme/substrate ratio of 1/100, with shaking for 2 hours at 37 °C. The gliadin peptic digest was lyophilized and further dissolved in 100 mM ammonium bicarbonate at 1 mg/ml. Trypsin (#T9201, Sigma-Aldrich) was added at an enzyme/substrate ratio of 1/100 and incubated with shaking for 4 hours at 37 °C. The reaction was stopped by boiling for 5 minutes. Identical conditions (minus substrate gliadin) were applied to generate a PTG negative control (PTG-CT) that was employed in some experiments to test the biological activity of the PTG-CT (Supplementary Fig. S3a,b). The PTG and PTG-CT were centrifuged at 4,000 rpm for 10 minutes, aliquoted, lyophilized, and stored frozen at –80 °C. PTG was resuspended at 10 mg/mL and used at a final concentration of 1 mg/mL, as previously reported^{5,39}.

Sodium L-lactate (#L7022, Sigma-Aldrich), and sodium butyrate (#B5887, Sigma-Aldrich) were resuspended at 1.5 mg/ml and 1.0 mg/ml respectively, in DMEM/F12, aliquoted and stored at –80 °C, and were used at a working concentration of 1.5 µg/mL and 1.0 µg/mL, respectively. Polysaccharide A (PSA) was purified from *Bacteroides fragilis* NCTC 9343 and provided by Dr. Dennis Kasper, Department of Microbiology and Immunobiology, Harvard Medical School, Boston, MA, USA, prepared as previously described⁷⁸. PSA was resuspended in sterile PBS at 100 mg/ml, stored at –80 °C, and used at a working concentration of 100 µg/mL.

PTG, PTG-CT, lactate, butyrate, and PSA were tested at working concentrations for endotoxin levels using the Limulus Amebocyte Lysate assay (QCL-1000, Lonza, USA) according to manufacturer's procedures. All the reagents had an endotoxin level ≤ 1.5 EU/mL. Lactate dehydrogenase (LDH) assay was employed to test the cytotoxicity of the generated reagents (CytoTox 96 Non-Radioactive Cytotoxicity Assay, #G1780, Promega, USA). Similar levels of LDH were detected for untreated and treated monolayers with the bacterial derived-molecules or PTG or PTG-CT (Supplementary Fig. S3c).

Duodenal organoid-derived monolayers and experimental procedures. Organoid-derived monolayers were established by seeding 1×10^5 single cells in 100 µl L-WRN/ISC medium per well on an uncoated polyester membrane transwell inserts with a 0.4 µm pore size (24 well plate, #3470, Corning, USA). The L-WRN/ISC medium was freshly supplemented with Y-27623 Rock inhibitor and changed every other day. TEER measurements and microscope direct observation were employed to monitor confluence. In order to promote cell differentiation and maturation, the confluent monolayers were apically treated with 5 µM DAPT (#565784, Calbiochem) in DMEM/F12 for 48 hours¹⁹, whereas basolateral media contained L-WRN/ISC medium only. In some experiments, monolayers were apically pre-treated, along with DAPT, with the following: lactate, butyrate, or PSA for 48 hours, followed by media change DMEM/F12 and subsequently challenged with PTG at 1 mg/mL⁵ for 4 hours. Basolateral supernatant was collected for analysis. Experiments were performed at least three times in triplicates.

Measurement of integrity and paracellular permeability of the monolayers. TEER was evaluated during development of the monolayers and after PTG challenge as a quantitative measure of barrier integrity⁷⁹. A dual planar electrode instrument (Endhom Evom, World Precision Instruments, USA) was employed according to manufacturer's directions. Data were expressed as resistance multiplied by the area ($\Omega \cdot \text{cm}^2$).

Paracellular permeability was evaluated by measuring the diffusion of two different molecular size neutral molecules: FITC-dextran, molecular weight of 4,000 Da (#FD4 Sigma-Aldrich) and FITC-PEG of 400 Da (#PG1-FC-400, Nanocs, USA). FITC-dextran or FITC-PEG was added apically at 1 mg/ml and measured in the basolateral media after 4 hours by spectrophotofluorimetry (Synergy 2, Biotek, USA) (485/528 nm excitation/emission wavelength), as previously reported⁸⁰.

Organoids' growth evaluation. To examine the organoids growth over time, NC and CD organoids were plated at 5×10^4 cells/mL and cultured for 7 days as previously described. Multiple fields per sample were acquired at 2, 4 and 7 days after plating using a bright field direct microscope (Invertoskop 40 C, Zeiss, Oberkochen, Germany). We calculated the area of the organoids (μm^2) in the captured microfield using ImageJ Software (National Institute of Health, USA) and then averaged the areas based on the total number of the measured organoids.

Immunofluorescence staining. Cells were fixed in 4% paraformaldehyde and directly stained based on standard protocols¹⁹. The monolayers and organoids images were acquired using the microscope Nikon C2 confocal and Nikon Eclipse 80i (Nikon, USA), respectively. The cells were co-stained with 4'-6'-diamino-2-phenylindole 1:1000 (DAPI) nuclear marker (blue). Antibodies: ZO1 Alexa Fluor 488 conjugate 1:100 (#339188, Invitrogen, USA) and cleaved caspase-3 (Asp175) 1:200 (#9661, Cell Signaling Technology, USA).

Propidium iodide staining. NC and CD organoids were collected, trypsinized and fixed in ethanol 66% accordingly to standards protocols. Propidium iodide staining was performed with Propidium Iodide Flow Cytometry Kit for Cell Cycle Analysis (#139418, Abcam, USA) following the manufacturer instructions. 2×10^4 cells per samples were acquired and analysis was performed on gated cells that excluded debris, apoptotic cells and doublet cells (Supplementary Fig. S2c,d).

Gene	Forward	Reverse
18S	AGAAACGGCTACCACATCCA	CCCTCCAATGGATCCTCGTT
ASCL2	GCGTGAAGCTGGTGAAGTGG	GGATGTACTCCACGGCTGAG
CCL24	ACATCATCCCTACGGGCTCT	CTGGGGTCGCCACAGAAC
CCL25	GGCCCTCATGCTGTAAAGAAG	TGCTGATGGGATTGCTAAACTT
CHGA	TAAAGGGGATACCAGGTGATG	TCGGAGTGTCTCAAAACATTCC
CLDN18	ACATGCTGGTGACTAACTTCTG	AAATGTGTACCTGGTCTGAACAG
CLDN2	PPH02779A (Qiagen)	
DEFA5	AGACAACCAGGACCTTGCTAT	GGAGAGGGACTCACGGGTAG
Haptoglobin (HP)	TTTCTGGCTGCTAAGTGG	AATGTCTTTCGCTGTGGC
IL37	TTCTTTGCATTAGCCTCATCCTT	CGTGCTGATTCTTTTGGGC
LGR5	PPH13346A (Qiagen)	
LYZ	CTTGTCTCCTTTCTGTACGG	CCCCTGTAGCCATCCATTCC
MUC2	GCCAGCTCATCAAGGACAG	GCAGGCATCGTAGTAGTGCTG
MUC5AC	CAGCACAAACCCTGTTTCAAA	GCGCACAGAGGATGACAGT
MUC6	CTGCCCTATACCAGCAATGGA	CTGACCCATGTACTTCCGCTC
MYC	GTCAAGAGGGCAACACACAAC	TTGGACGGACAGGATGTATGC
NLRP6	CCTACCAGTTTCATCGACCAGA	CTCAGCAGTCCGAAGAGGAA
OLFM4	ACTGTCCGAATTGACATCATGG	TTCTGAGCTTCCACAAAATCTC
PCNA	CCTGCTGGGATATTAGCTCCA	CAGCGGTAGGTGTCGAAGC
SI	TCCAGCTACTACTCGTGTGAC	CCCTCTGTGGGAATTGTTCTG
SMOC2	ATGACGACGGCACCTACAG	TCGCGTTGGGTAACCTTTTCA
TFF1	CCCTCCCAGTGTGCAAATAAG	GAACGGTGTCTCGTGAACAG
TNFRSF25	PPH00349B (Qiagen)	
TP53	ACTTGTCTGCTCTTGAAGCTAC	GATGCGGAGAATCTTTGGAACA
ZO1	CAACATACAGTGACGCTTCACA	CACTATTGACGTTTCCCCACTC

Table 1. Oligonucleotide primers for quantitative RT-PCR analysis.

Fluorescence activated cell sorting and analysis (FACS). Staining for Ki67 and phospho-histone H3 (H3P) was performed on trypsinized cells from NC and CD organoids previously fixed in formaldehyde 4% and permeabilized in methanol 90%. Cells were then washed in PBS, incubated with anti-Ki67 antibody (FITC-conjugate, #16667, Abcam) and H3P (Pacific Blue conjugate, #8552, Cell Signaling Technology, USA) in Bovine Serum Albumin 0.5% in PBS (#A7906, Sigma-Aldrich) and washed twice. 10^5 cells per samples were acquired and analysis was performed on gated cells that excluded debris and double positive (Ki67⁺H3P⁺) representative of cells that entered mitosis. Data were acquired with BD FACS Calibur flow cytometer instrument. Analysis was performed with BD CellQuestPro software.

Gene expression analysis. RNA extraction from organoids, monolayers and duodenal were carried out in TRIzol reagent and total RNA was purified using Zymo-Spin column (#R2050, Zymo Research, USA), according to manufacturer's protocol. cDNA was generated from RNA using the Maxima H minus first strand cDNA synthesis kit (#K1652, Thermo Fischer Scientific). SYBR Green reagent (Applied Biosystems/Life Technologies, US) and CFX Connect Real-time PCR detection system (Bio-Rad, USA) were used for gene expression analysis (quantitative RT-PCR). The 18S gene expression was used as an internal control. The results were expressed as the fold change over sample control applying the C_T method ($2^{-\Delta\Delta C_T}$)⁸¹. The oligonucleotide primers used were designed by the MGH primer bank (Boston, MA, USA) and synthesized by IDT (San Jose, CA, USA) or purchased from Qiagen, (Limburg, Netherlands) (Table 1).

RNA-seq analysis: total RNA isolated as described was subjected to polyA selection, followed by NGS library construction using NEBNext Ultra Directional RNA Library Prep Kit for Illumina (New England Biolabs, USA). Sequencing was performed on an Illumina HiSeq 2500 instrument and reads were mapped to the human reference genome (hg19 build) using STAR⁸², resulting in a range of 30–50 million aligned single-end 50 bp reads per sample. Read counts over transcripts were calculated using HTSeq v.0.6.0⁸³ based on the most current Ensembl annotation file for hg19. Genes with RPKM (Reads Per Kilobase per Million mapped reads) greater than 1.0 were considered transcriptionally active. Functional annotation analysis was performed on differentially expressed genes (two-fold change and FDR < 0.05 value) using DAVID v6.7 [<https://david-d.ncicrf.gov/>]^{22,23}. Functional gene set enrichment analysis (GSEA) was performed on the whole-transcriptome expression values using GSEA²⁴ comparison against Hallmark gene sets with default parameters and a nominal p-value cutoff of 0.01.

Haptoglobin (HP) genotyping. DNA isolation was performed by silica-based spin-column (#69504, Qiagen, USA), according to manufacturer's instructions. Haptoglobin 2 genotyping was performed using specific primers (Table 1) designed in exon 2 and exon 5 of HP1 corresponding to exons 2 and 7 of HP2⁸⁴ amplified by high fidelity PCR system (Arktik Thermal Cycler, Thermo Fisher Scientific). After PCR, the amplicons were run

on a 1% agarose gel and read under a UV bulb (GeneFlash, Syngene, USA). The band size difference allowed differentiation of the two genotypes (HP1: 2.5 kb and HP2: 5.3 kb).

Cytokine analysis. A pro-inflammatory panel of cytokines including IL6, IL8, IL15, TNF, and IFN γ was evaluated in the basolateral medium of treated monolayers using a multiplex electrochemiluminescence assay (#K15067L-2, MesoScale Discovery, USA), according to manufacturer's instructions. The data analysis was performed using the MSD Discovery Workbench 4.0 software.

Statistics. Analysis of RNA-seq data was performed using EdgeR package (version 3.8.6)⁸⁵ based on the criteria of more than a two-fold change in expression value and FDR (Benjamini-Hochberg) less than a 0.05 value and the hypergeometric enrichment test. All other statistical analyses were performed using the software GraphPad Prism 7.0 (GraphPad Software). Normal distribution of the data set was evaluated using the D'Agostino & Pearson test. Parametric data were analyzed by Student's t-test and nonparametric variables by Mann-Whitney test (2 groups). Data represent average \pm SEM. A significance level of 0.1% ($p < 0.001$), 1% ($p < 0.01$) and 5% ($p < 0.05$) was adopted.

Study approval. All protocols and samples collections were approved by the Massachusetts General Hospital Institutional Review Board (#2014P000198) and performed in accordance with relevant guidelines and regulations. All patients gave written informed consent prior to study inclusion.

Data Availability

RNA-seq data generated for this study were uploaded at NCBI-GEO databank, Accession Number: GSE113492. All datasets generated and/or analyzed during the current study are available from the corresponding author on reasonable request.

References

- Leonard, M. M., Sapone, A., Catassi, C. & Fasano, A. Celiac Disease and Nonceliac Gluten Sensitivity: A Review. *JAMA* **318**, 647–656, <https://doi.org/10.1001/jama.2017.9730> (2017).
- Husby, S. *et al.* European Society for Pediatric Gastroenterology, Hepatology, and Nutrition guidelines for the diagnosis of coeliac disease. *J Pediatr Gastroenterol Nutr* **54**, 136–160, <https://doi.org/10.1097/MPG.0b013e31821a23d0> (2012).
- Dickson, B. C., Streutker, C. J. & Chetty, R. Coeliac disease: an update for pathologists. *J Clin Pathol* **59**, 1008–1016, <https://doi.org/10.1136/jcp.2005.035345> (2006).
- Fasano, A. Zonulin and its regulation of intestinal barrier function: the biological door to inflammation, autoimmunity, and cancer. *Physiol Rev* **91**, 151–175, <https://doi.org/10.1152/physrev.00003.2008> (2011).
- Drago, S. *et al.* Gliadin, zonulin and gut permeability: Effects on celiac and non-celiac intestinal mucosa and intestinal cell lines. *Scand J Gastroenterol* **41**, 408–419, <https://doi.org/10.1080/00365520500235334> (2006).
- Hollon, J. *et al.* Effect of gliadin on permeability of intestinal biopsy explants from celiac disease patients and patients with non-celiac gluten sensitivity. *Nutrients* **7**, 1565–1576, <https://doi.org/10.3390/nu7031565> (2015).
- Leffler, D. A., Green, P. H. & Fasano, A. Extraintestinal manifestations of coeliac disease. *Nat Rev Gastroenterol Hepatol* **12**, 561–571, <https://doi.org/10.1038/nrgastro.2015.131> (2015).
- Lammers, K. M. *et al.* Identification of a novel immunomodulatory gliadin peptide that causes interleukin-8 release in a chemokine receptor CXCR3-dependent manner only in patients with coeliac disease. *Immunology* **132**, 432–440, <https://doi.org/10.1111/j.1365-2567.2010.03378.x> (2011).
- Di Sabatino, A. *et al.* Epithelium derived interleukin 15 regulates intraepithelial lymphocyte Th1 cytokine production, cytotoxicity, and survival in coeliac disease. *Gut* **55**, 469–477, <https://doi.org/10.1136/gut.2005.068684> (2006).
- Serena, G., Camhi, S., Sturgeon, C., Yan, S. & Fasano, A. The Role of Gluten in Celiac Disease and Type 1 Diabetes. *Nutrients* **7**, 7143–7162, <https://doi.org/10.3390/nu7095329> (2015).
- Fasano, A. & Catassi, C. Current approaches to diagnosis and treatment of celiac disease: an evolving spectrum. *Gastroenterology* **120**, 636–651 (2001).
- Catassi, C. *et al.* Natural history of celiac disease autoimmunity in a USA cohort followed since 1974. *Ann Med* **42**, 530–538, <https://doi.org/10.3109/07853890.2010.514285> (2010).
- Collado, M. C., Donat, E., Ribes-Koninckx, C., Calabuig, M. & Sanz, Y. Specific duodenal and faecal bacterial groups associated with paediatric coeliac disease. *J Clin Pathol* **62**, 264–269, <https://doi.org/10.1136/jcp.2008.061366> (2009).
- Cukrowska, B. *et al.* Intestinal epithelium, intraepithelial lymphocytes and the gut microbiota - Key players in the pathogenesis of celiac disease. *World J Gastroenterol* **23**, 7505–7518, <https://doi.org/10.3748/wjg.v23.i42.7505> (2017).
- Selitto, M. *et al.* Proof of concept of microbiome-metabolome analysis and delayed gluten exposure on celiac disease autoimmunity in genetically at-risk infants. *PLoS One* **7**, e33387, <https://doi.org/10.1371/journal.pone.0033387> (2012).
- Serena, G. *et al.* Proinflammatory cytokine interferon- γ and microbiome-derived metabolites dictate epigenetic switch between forkhead box protein 3 isoforms in coeliac disease. *Clin Exp Immunol* **187**, 490–506, <https://doi.org/10.1111/cei.12911> (2017).
- Marietta, E. V., David, C. S. & Murray, J. A. Important lessons derived from animal models of celiac disease. *Int Rev Immunol* **30**, 197–206, <https://doi.org/10.3109/08830185.2011.598978> (2011).
- Jung, P. *et al.* Isolation and *in vitro* expansion of human colonic stem cells. *Nat Med* **17**, 1225–1227, <https://doi.org/10.1038/nm.2470> (2011).
- Senger, S. *et al.* Human Fetal-Derived Enterospheres Provide Insights on Intestinal Development and a Novel Model to Study Necrotizing Enterocolitis (NEC). *Cell Mol Gastroenterol Hepatol* **5**, 549–568, <https://doi.org/10.1016/j.jcmgh.2018.01.014> (2018).
- Lammers, K. M. *et al.* Gliadin Induces Neutrophil Migration via Engagement of the Formyl Peptide Receptor, FPR1. *PLoS One* **10**, e0138338, <https://doi.org/10.1371/journal.pone.0138338> (2015).
- Senger, S. *et al.* Celiac Disease Histopathology Recapitulates Hedgehog Downregulation, Consistent with Wound Healing Processes Activation. *PLoS One* **10**, e0144634, <https://doi.org/10.1371/journal.pone.0144634> (2015).
- Huang, D. W. *et al.* DAVID Bioinformatics Resources: expanded annotation database and novel algorithms to better extract biology from large gene lists. *Nucleic Acids Res* **35**, W169–175, <https://doi.org/10.1093/nar/gkm415> (2007).
- Huang, D. W. *et al.* The DAVID Gene Functional Classification Tool: a novel biological module-centric algorithm to functionally analyze large gene lists. *Genome Biol* **8**, R183, <https://doi.org/10.1186/gb-2007-8-9-r183> (2007).
- Subramanian, A. *et al.* Gene set enrichment analysis: a knowledge-based approach for interpreting genome-wide expression profiles. *Proc Natl Acad Sci USA* **102**, 15545–15550, <https://doi.org/10.1073/pnas.0506580102> (2005).
- Fedi, P. *et al.* Isolation and biochemical characterization of the human Dkk-1 homologue, a novel inhibitor of mammalian Wnt signaling. *J Biol Chem* **274**, 19465–19472 (1999).

26. Tamura, A. & Tsukita, S. Paracellular barrier and channel functions of TJ claudins in organizing biological systems: advances in the field of barrierology revealed in knockout mice. *Semin Cell Dev Biol* **36**, 177–185, <https://doi.org/10.1016/j.semcdb.2014.09.019> (2014).
27. Fanning, A. S., Jameson, B. J., Jesaitis, L. A. & Anderson, J. M. The tight junction protein ZO-1 establishes a link between the transmembrane protein occludin and the actin cytoskeleton. *J Biol Chem* **273**, 29745–29753 (1998).
28. Pizzuti, D. *et al.* Transcriptional downregulation of tight junction protein ZO-1 in active coeliac disease is reversed after a gluten-free diet. *Dig Liver Dis* **36**, 337–341, <https://doi.org/10.1016/j.dld.2004.01.013> (2004).
29. Schumann, M. *et al.* Defective tight junctions in refractory celiac disease. *Ann N Y Acad Sci* **1258**, 43–51, <https://doi.org/10.1111/j.1749-6632.2012.06565.x> (2012).
30. Dotti, I. *et al.* Alterations in the epithelial stem cell compartment could contribute to permanent changes in the mucosa of patients with ulcerative colitis. *Gut* **66**, 2069–2079, <https://doi.org/10.1136/gutjnl-2016-312609> (2017).
31. Piscaglia, A. C. *et al.* Circulating hematopoietic stem cells and putative intestinal stem cells in coeliac disease. *J Transl Med* **13**, 220, <https://doi.org/10.1186/s12967-015-0591-0> (2015).
32. Shalimar, D. M. *et al.* Mechanism of villous atrophy in celiac disease: role of apoptosis and epithelial regeneration. *Arch Pathol Lab Med* **137**, 1262–1269, <https://doi.org/10.5858/arpa.2012-0354-OA> (2013).
33. Schumann, M., Siegmund, B., Schulzke, J. D. & Fromm, M. Celiac Disease: Role of the Epithelial Barrier. *Cell Mol Gastroenterol Hepatol* **3**, 150–162, <https://doi.org/10.1016/j.jcmgh.2016.12.006> (2017).
34. Crowley, L. C., Marfell, B. J., Scott, A. P. & Waterhouse, N. J. Quantitation of Apoptosis and Necrosis by Annexin V Binding, Propidium Iodide Uptake, and Flow Cytometry. *Cold Spring Harb Protoc* **2016**, <https://doi.org/10.1101/pdb.prot087288> (2016).
35. Riccardi, C. & Nicoletti, I. Analysis of apoptosis by propidium iodide staining and flow cytometry. *Nat Protoc* **1**, 1458–1461, <https://doi.org/10.1038/nprot.2006.238> (2006).
36. Fang, L., Adkins, B., Deyev, V. & Podack, E. R. Essential role of TNF receptor superfamily 25 (TNFRSF25) in the development of allergic lung inflammation. *J Exp Med* **205**, 1037–1048, <https://doi.org/10.1084/jem.20072528> (2008).
37. Li, Q. *et al.* Upregulated p53 expression activates apoptotic pathways in wild-type p53-bearing mesothelioma and enhances cytotoxicity of cisplatin and pemetrexed. *Cancer Gene Ther* **19**, 218–228, <https://doi.org/10.1038/cgt.2011.86> (2012).
38. Maeda, N., Yang, F., Barnett, D. R., Bowman, B. H. & Smithies, O. Duplication within the haptoglobin Hp2 gene. *Nature* **309**, 131–135 (1984).
39. Lammers, K. M. *et al.* Gliadin induces an increase in intestinal permeability and zonulin release by binding to the chemokine receptor CXCR3. *Gastroenterology* **135**, 194–204.e193, <https://doi.org/10.1053/j.gastro.2008.03.023> (2008).
40. Tripathi, A. *et al.* Identification of human zonulin, a physiological modulator of tight junctions, as prehaptoglobin-2. *Proc Natl Acad Sci USA* **106**, 16799–16804, <https://doi.org/10.1073/pnas.0906773106> (2009).
41. VanDussen, K. L. *et al.* Development of an enhanced human gastrointestinal epithelial culture system to facilitate patient-based assays. *Gut* **64**, 911–920, <https://doi.org/10.1136/gutjnl-2013-306651> (2015).
42. Capozzi, A. *et al.* Modulatory Effect of Gliadin Peptide 10-mer on Epithelial Intestinal CACO-2 Cell Inflammatory Response. *PLoS One* **8**, e66561, <https://doi.org/10.1371/journal.pone.0066561> (2013).
43. Mamone, G. *et al.* Susceptibility to transglutaminase of gliadin peptides predicted by a mass spectrometry-based assay. *FEBS Lett* **562**, 177–182, [https://doi.org/10.1016/S0014-5793\(04\)00231-5](https://doi.org/10.1016/S0014-5793(04)00231-5) (2004).
44. Willemsen, L. E., Hoetjes, J. P., van Deventer, S. J. & van Tol, E. A. Abrogation of IFN-gamma mediated epithelial barrier disruption by serine protease inhibition. *Clin Exp Immunol* **142**, 275–284, <https://doi.org/10.1111/j.1365-2249.2005.02906.x> (2005).
45. De Palma, G. *et al.* Intestinal dysbiosis and reduced immunoglobulin-coated bacteria associated with coeliac disease in children. *BMC Microbiol* **10**, 63, <https://doi.org/10.1186/1471-2180-10-63> (2010).
46. Troy, E. B. & Kasper, D. L. Beneficial effects of *Bacteroides fragilis* polysaccharides on the immune system. *Front Biosci (Landmark Ed)* **15**, 25–34 (2010).
47. Jiang, F. *et al.* The symbiotic bacterial surface factor polysaccharide A on *Bacteroides fragilis* inhibits IL-1 β -induced inflammation in human fetal enterocytes via toll receptors 2 and 4. *PLoS One* **12**, e0172738, <https://doi.org/10.1371/journal.pone.0172738> (2017).
48. Wang, Q. *et al.* A bacterial carbohydrate links innate and adaptive responses through Toll-like receptor 2. *J Exp Med* **203**, 2853–2863, <https://doi.org/10.1084/jem.20062008> (2006).
49. Mu, Q., Kirby, J., Reilly, C. M. & Luo, X. M. Leaky Gut As a Danger Signal for Autoimmune Diseases. *Front Immunol* **8**, 598, <https://doi.org/10.3389/fimmu.2017.00598> (2017).
50. Buckley, A. & Turner, J. R. Cell Biology of Tight Junction Barrier Regulation and Mucosal Disease. *Cold Spring Harb Perspect Biol* **10**, <https://doi.org/10.1101/cshperspect.a029314> (2018).
51. Pietz, G. *et al.* Immunopathology of childhood celiac disease—Key role of intestinal epithelial cells. *PLoS One* **12**, e0185025, <https://doi.org/10.1371/journal.pone.0185025> (2017).
52. Szakál, D. N. *et al.* Mucosal expression of claudins 2, 3 and 4 in proximal and distal part of duodenum in children with coeliac disease. *Virchows Arch* **456**, 245–250, <https://doi.org/10.1007/s00428-009-0879-7> (2010).
53. Sapone, A. *et al.* Divergence of gut permeability and mucosal immune gene expression in two gluten-associated conditions: celiac disease and gluten sensitivity. *BMC Med* **9**, 23, <https://doi.org/10.1186/1741-7015-9-23> (2011).
54. Hære, P. *et al.* Long-term mucosal recovery and healing in celiac disease is the rule - not the exception. *Scand J Gastroenterol* **51**, 1439–1446, <https://doi.org/10.1080/00365521.2016.1218540> (2016).
55. Forsberg, G. *et al.* Presence of bacteria and innate immunity of intestinal epithelium in childhood celiac disease. *Am J Gastroenterol* **99**, 894–904, <https://doi.org/10.1111/j.1572-0241.2004.04157.x> (2004).
56. Xuan, W., Qu, Q., Zheng, B., Xiong, S. & Fan, G. H. The chemotaxis of M1 and M2 macrophages is regulated by different chemokines. *J Leukoc Biol* **97**, 61–69, <https://doi.org/10.1189/jlb.1A0314-170R> (2015).
57. Mizuno, S. *et al.* CCR9+ plasmacytoid dendritic cells in the small intestine suppress development of intestinal inflammation in mice. *Immunol Lett* **146**, 64–69, <https://doi.org/10.1016/j.imlet.2012.05.001> (2012).
58. Trivedi, P. J. *et al.* Intestinal CCL25 expression is increased in colitis and correlates with inflammatory activity. *J Autoimmun* **68**, 98–104, <https://doi.org/10.1016/j.jaut.2016.01.001> (2016).
59. Olausson, R. W. *et al.* Reduced chemokine receptor 9 on intraepithelial lymphocytes in celiac disease suggests persistent epithelial activation. *Gastroenterology* **132**, 2371–2382, <https://doi.org/10.1053/j.gastro.2007.04.023> (2007).
60. Quirk, S. & Agrawal, D. K. Immunobiology of IL-37: mechanism of action and clinical perspectives. *Expert Rev Clin Immunol* **10**, 1703–1709, <https://doi.org/10.1586/1744666X.2014.971014> (2014).
61. Song, L. *et al.* Glucocorticoid regulates interleukin-37 in systemic lupus erythematosus. *J Clin Immunol* **33**, 111–117, <https://doi.org/10.1007/s10875-012-9791-z> (2013).
62. Imaeda, H. *et al.* Epithelial expression of interleukin-37b in inflammatory bowel disease. *Clin Exp Immunol* **172**, 410–416, <https://doi.org/10.1111/cei.12061> (2013).
63. Nold, M. F. *et al.* IL-37 is a fundamental inhibitor of innate immunity. *Nat Immunol* **11**, 1014–1022, <https://doi.org/10.1038/ni.1944> (2010).
64. Luo, Y. *et al.* Suppression of antigen-specific adaptive immunity by IL-37 via induction of tolerogenic dendritic cells. *Proc Natl Acad Sci USA* **111**, 15178–15183, <https://doi.org/10.1073/pnas.1416714111> (2014).
65. Levy, M., Shapiro, H., Thaiss, C. A. & Elinav, E. NLRP6: A Multifaceted Innate Immune Sensor. *Trends Immunol* **38**, 248–260, <https://doi.org/10.1016/j.it.2017.01.001> (2017).

66. Mention, J. J. *et al.* Interleukin 15: a key to disrupted intraepithelial lymphocyte homeostasis and lymphomagenesis in celiac disease. *Gastroenterology* **125**, 730–745 (2003).
67. Reinecker, H. C., MacDermott, R. P., Mirau, S., Dignass, A. & Podolsky, D. K. Intestinal epithelial cells both express and respond to interleukin 15. *Gastroenterology* **111**, 1706–1713 (1996).
68. Maiuri, L. *et al.* Interleukin 15 mediates epithelial changes in celiac disease. *Gastroenterology* **119**, 996–1006 (2000).
69. Vieira, S. M., Pagovich, O. E. & Kriegel, M. A. Diet, microbiota and autoimmune diseases. *Lupus* **23**, 518–526, <https://doi.org/10.1177/096120313501401> (2014).
70. Vidyasagar, S., Barmeyer, C., Geibel, J., Binder, H. J. & Rajendran, V. M. Role of short-chain fatty acids in colonic HCO₃ secretion. *Am J Physiol Gastrointest Liver Physiol* **288**, G1217–1226, <https://doi.org/10.1152/ajpgi.00415.2004> (2005).
71. Inan, M. S. *et al.* The luminal short-chain fatty acid butyrate modulates NF-kappaB activity in a human colonic epithelial cell line. *Gastroenterology* **118**, 724–734 (2000).
72. Klampfer, L., Huang, J., Sasazuki, T., Shirasawa, S. & Augenlicht, L. Inhibition of interferon gamma signaling by the short chain fatty acid butyrate. *Mol Cancer Res* **1**, 855–862 (2003).
73. Yan, H. & Ajuwon, K. M. Butyrate modifies intestinal barrier function in IPEC-J2 cells through a selective upregulation of tight junction proteins and activation of the Akt signaling pathway. *PLoS One* **12**, e0179586, <https://doi.org/10.1371/journal.pone.0179586> (2017).
74. Duncan, S. H., Louis, P. & Flint, H. J. Lactate-utilizing bacteria, isolated from human feces, that produce butyrate as a major fermentation product. *Appl Environ Microbiol* **70**, 5810–5817, <https://doi.org/10.1128/AEM.70.10.5810-5817.2004> (2004).
75. Orlando, A., Linsalata, M., Notarnicola, M., Tutino, V. & Russo, F. Lactobacillus GG restoration of the gliadin induced epithelial barrier disruption: the role of cellular polyamines. *BMC Microbiol* **14**, 19, <https://doi.org/10.1186/1471-2180-14-19> (2014).
76. Resta-Lenert, S. & Barrett, K. E. Probiotics and commensals reverse TNF-alpha- and IFN-gamma-induced dysfunction in human intestinal epithelial cells. *Gastroenterology* **130**, 731–746, <https://doi.org/10.1053/j.gastro.2005.12.015> (2006).
77. Round, J. L. & Mazmanian, S. K. Inducible Foxp3+ regulatory T-cell development by a commensal bacterium of the intestinal microbiota. *Proc Natl Acad Sci USA* **107**, 12204–12209, <https://doi.org/10.1073/pnas.0909122107> (2010).
78. Baumann, H., Tzianabos, A. O., Brisson, J. R., Kasper, D. L. & Jennings, H. J. Structural elucidation of two capsular polysaccharides from one strain of *Bacteroides fragilis* using high-resolution NMR spectroscopy. *Biochemistry* **31**, 4081–4089 (1992).
79. Srinivasan, B. *et al.* TEER measurement techniques for *in vitro* barrier model systems. *J Lab Autom* **20**, 107–126, <https://doi.org/10.1177/2211068214561025> (2015).
80. Fiorentino, M. *et al.* Helicobacter pylori-induced disruption of monolayer permeability and proinflammatory cytokine secretion in polarized human gastric epithelial cells. *Infect Immun* **81**, 876–883, <https://doi.org/10.1128/IAI.01406-12> (2013).
81. Schmittgen, T. D. & Livak, K. J. Analyzing real-time PCR data by the comparative C(T) method. *Nat Protoc* **3**, 1101–1108 (2008).
82. Dobin, A. *et al.* STAR: ultrafast universal RNA-seq aligner. *Bioinformatics* **29**, 15–21, <https://doi.org/10.1093/bioinformatics/bts635> (2013).
83. Anders, S., Pyl, P. T. & Huber, W. HTSeq—a Python framework to work with high-throughput sequencing data. *Bioinformatics* **31**, 166–169, <https://doi.org/10.1093/bioinformatics/btu638> (2015).
84. Koch, W. *et al.* Genotyping of the common haptoglobin Hp 1/2 polymorphism based on PCR. *Clin Chem* **48**, 1377–1382 (2002).
85. Robinson, M. D., McCarthy, D. J. & Smyth, G. K. edgeR: a Bioconductor package for differential expression analysis of digital gene expression data. *Bioinformatics* **26**, 139–140, <https://doi.org/10.1093/bioinformatics/btp616> (2010).

Acknowledgements

This work was partially supported by the Egan Family Foundation and the National Institutes of Health (NIH) Grants RO1DK104344 and 1U19AI082655. The authors thank Susie Flaherty for the editing of the manuscript. We thank the clinical research coordinators, Stephanie Camhi and Rosie Lima, and the medical staff at Massachusetts General Hospital (MGH, Boston, MA) in facilitating the collection of samples. We are grateful to Weishu Zhu for technical help with culturing the organoids; the MGH Peptide/Protein Core Facility for lyophilizing of reagents; Harvard Catalyst (The Harvard Clinical and Translational Science Center) for consulting on biostatistics; and MGH Next-Generation Sequencing Core at MGH for RNA sequencing of samples. We thank Professor Dennis Kasper (Department of Microbiology and Immunobiology, Harvard Medical School, Boston, MA) for providing the polysaccharide A employed in this study.

Author Contributions

R.F. designed and conducted the experiments, analyzed the data, and wrote the manuscript. R.S. conceived the RNA-seq data analysis. A.A. and M.C. analyzed the RNA-seq data. G.S. and L.I. conducted experiments. A.S. contributed to the generation of the samples. S.S. and A.F. conceived and designed the study, analyzed the data, and wrote the manuscript. All authors had access to the data and have reviewed and approved the final paper.

Additional Information

Supplementary information accompanies this paper at <https://doi.org/10.1038/s41598-019-43426-w>.

Competing Interests: R.F., G.S., L.I., R.S., M.C. declare no competing interests. S.S. declares the following financial relationship: stock holder of Array Biopharma Inc.; A.A. is currently employed at PatientsLikeMe, Inc., Cambridge; A.S. is currently employed at Takeda Pharmaceuticals International Co. as associate medical director and received consultancy fees from Inova Diagnostics Inc.; A.F. declares the following financial relationships: stock holder of Alba Therapeutics, advisory board committee member at Axial Biotherapeutics and uBiome; consultant at Inova Diagnostics Inc. and Innovate Biopharmaceuticals, Inc., speaker agreement with Mead Johnson Nutrition.

Publisher's note: Springer Nature remains neutral with regard to jurisdictional claims in published maps and institutional affiliations.



Open Access This article is licensed under a Creative Commons Attribution 4.0 International License, which permits use, sharing, adaptation, distribution and reproduction in any medium or format, as long as you give appropriate credit to the original author(s) and the source, provide a link to the Creative Commons license, and indicate if changes were made. The images or other third party material in this article are included in the article's Creative Commons license, unless indicated otherwise in a credit line to the material. If material is not included in the article's Creative Commons license and your intended use is not permitted by statutory regulation or exceeds the permitted use, you will need to obtain permission directly from the copyright holder. To view a copy of this license, visit <http://creativecommons.org/licenses/by/4.0/>.

© The Author(s) 2019